JOURNAL OF COMPUTATIONAL PHYSICS 53, 240–265 (1984)

A Lagrangian Method for the Shallow Water Equations Based on a Voronoi Mesh—One Dimensional Results

JEFFREY M. AUGENBAUM*

Courant Institute of Mathematical Sciences, New York University, New York, New York 10012

Received October 14, 1982; revised April 19, 1983

A Lagrangian method for the Shallow Water equations in one dimension is presented. The method is based on the following idea. Place N points on a line to represent the fluid. Each point represents all the fluid that is closer to this point than to any other. This partitions the line into intervals. The principle of Least Action yields a set of difference equations which can be easily solved at each time step to give new values for the height and velocity of the fluid particles in each interval. The points are then moved to their new locations and the intervals reconstructed. In the event that two points get too close to each other, consider the points to have collided. The collision is treated as an inelastic collision and the two points are merged into one, according to certain conservation laws. It is then possible to handle flows with shocks by modelling a shock as a collision between two particles. That is, a shock is thought of as one fluid particle overtaking another one and colliding with it. The results of this method on the Dam-Breaking problem are presented. The solution is compared to the exact solution and to a solution by the Random Choice Method.

1. INTRODUCTION

In this paper we introduce a new numerical method for the treatment of the shallow water equations. The method is based on a Lagrangian representation of the fluid. That is, the coordinates, velocities and height of N fluid markers are stored and updated at each time step.

The main advantage of a Lagrangian formulation is that the conservation equations take their simplest form. In particular, the nonlinear convection terms $\bar{u} \cdot \nabla \bar{u}$ do not appear explicitly.

Despite this advantage, the Lagrangian approach has a fundamental difficulty associated with large deformations generated by typical fluid motions. Fluid particles which are close together at time $t = 0$ may become farther and farther apart as time evolves. Conversely, fluid particles that are far apart may come closer together and even collide. A computational mesh that moves with the fluid becomes increasingly distorted, and the difference approximations to derivatives become worse and worse.

Various Lagrangian schemes are described in the literature. One of the most

* Present affiliation: NASA-Goddard Space Flight Center, Code 911, Greenbelt, Maryland 20771.

0021-9991/84 $3.00

successful is the Particle in Cell Method (PIC) [7]. In this method, the flow is represented by large numbers of particles carrying mass, momentum, and energy. The particles are accelerated by a pressure gradient determined by counting particles in a fixed mesh.

A Lagrangian scheme that deals with the difficulty of a deforming mesh is the ALE Technique [8]. In this method a computational mesh deforms with the fluid, but the deformation is opposed by a relaxation process which tends to preserve the regularity of the mesh.

Another approach is the Free Lagrangian Method proposed by Peskin [11] and others [4, 16]. The Free Lagrangian Method deals will the problem of large deformation in a different way. At each time step, the fluid markers find their natural neighbors. This is accomplished by assigning to each fluid marker the region of space consisting of points which are closer to that marker than to any other. Thus the fluid markers generate a natural partition of the domain into convex polygons, if the domain is two-dimensional, or into convex polyhedra, if its is three dimensional. The mesh so generated is known as a Voronoi mesh [17]. For this reason, the fluid markers will be called generating points.

Two generating points are considered neighbors if their polyhedra have a face of nonzero area in common. As the generating points move, the polyhedra deform continuously, but a given generating point is free to lose old neighbors and acquire new ones. These changes in structure occur continuously in the following sense. Let A_{jk} be the area of the face in common between polyhedra j and k when there is such a face. Otherwise, set $A_{jk} = 0$. Then A_{jk} is a continuous function of the coordinates of the generating points. Since the fluid markers find their natural neighbors at each time step, there is no tendency for the distance between neighbors to increase with time, and the difficulty of large deformations is overcome.

Peskin has implemented a Free Lagrangian Method for the case of plane incompressible flow, while Dukowicz and Trease have applied such methods to compressible flow problems [4, 16]. This method also is naturally suited to the shallow water equations. That is the subject of the present work. Each column of fluid is made up of a polygonal base with area A_j and a height H_j. The constraint of incompressibility is that the total mass of an element $m_k = \rho A_k H_k = \text{constant}$, where $\rho = \text{density}$. Thus the height is free to adjust as long as the base compensates for the changes in height. The shallow water theory (Stoker [15]) tells us that the motion of fluid in a cell is determined by the motion of fluid in the polygonal base. Thus the motion is essentially two dimensional. This allows us to write Lagrange's equations of motion for the generating points.

In one dimension the equations simplify considerably. This discussion is presented in the present paper as a prelude to the various generalizations to be discussed in the following paper (Augenbaum [2]). In the first few sections we derive the discrete equations (Sections 2 and 3) and then compare them to a more standard derivation, thus establishing the second-order spatial accuracy of the method in Lagrangian coordinates (Section 5). We then modify the scheme to handle the case of shocks by treating a shock as a collision between generating points. When two generating points

get too close to each other we treat them as if an inelastic collision has occured and merge the two points into one averaged point according to certain conservation laws. This procedure provides the dissipation of energy that is caused by the shock (Section 6). The loss of resolution that results from this procedure is appropriate to the dissipative nature of shocks. Finally, we present the results of this method on the dam-breaking problem (Section 9).

In the following paper [2] we generalize the method to the case of flow on a rotating sphere. Other Lagrangian methods that deal with the problem of large deformations can be found in Fritts and Boris [5].

2. Discrete Shallow Water Equations in One Space Dimension for Shock-Free Flows

In this section we describe the discrete approximation to the shallow water equations in one space dimension. These equations are derived in Stoker [5]. We recall them for the readers convenience,

$$\frac{Dh}{Dt} + h\frac{\partial u}{\partial x} = 0, \qquad \frac{Du}{Dt} + g\frac{\partial h}{\partial x} = 0, \tag{2.1}$$

where

$$\frac{D}{Dt} = \frac{\partial}{\partial t} + u\frac{\partial}{\partial x}$$

and

$h = h(x, t) =$ height of fluid,

$u = u(x, t) =$ horizontal velocity,

$g =$ gravitation constant.

We remark that we follow the usual convention of using small letters to denote Eulerian variables and capital letters to denote Lagrangian variables.

Assume that we have an interval on the line $a \leqslant x \leqslant b$ containing fluid with a free surface height $h(x)$ such that $\max[h(x)] \ll b - a$. We then place N fluid markers X_k such that

$$a < X_1 < X_2 < \cdots < X_k < X_{k+1} < \cdots < X_N < b.$$

In this way we partition the interval (a, b) into smaller intervals I_k so that each particle (fluid marker), X_k, represents all the fluid that is closer to X_k than to any other fluid point.

Each interval I_k is given by the formula

$$I_k = \left(\frac{X_{k-1} + X_k}{2}, \frac{X_k + X_{k+1}}{2}\right), \qquad 1 < k < N.$$

The boundary intervals are given by

$$I_1 = \left(a, \frac{X_1 + X_2}{2}\right), \qquad I_N = \left(\frac{X_{N-1} + X_N}{2}, b\right).$$

For purposes of generalization to higher dimensions it is worth noting that

$$I_k = \bigcap_{\substack{j=1 \\ j \neq k}}^{N} \{x : x \in (a, b) \text{ and } |x - X_k| \leqslant |x - X_j|\}.$$

To each interval, I_k, we associate its length L_k, and a height H_k. The area of any interval is given by

$$A_k = L_k H_k$$

and therefore its mass is

$$m_k = \rho(L_k H_k), \tag{2.2}$$

where $\rho =$ density. We remark that the units we use here are $m =$ mass/length and $\rho =$ mass/vol.

Equations of motion. First, since we are concerned with the time evolution of the fluid particles, all the quantities defined above are functions of time.

Incompressibility. Since the fluid is incompressible we have

$$m_j(t) = \rho L_j(t)\, H_j(t) = \text{const} = m_j(0) = m_j^0. \tag{2.3}$$

This implicitly defines H_j as a function of $(X_1, \ldots, X_N)$, i.e., $H_j = m_j/\rho L_j$. Recall that the L_j are determined by $(X_1, \ldots, X_N)$.

Lagrangian Dynamics. We construct a Lagrangian for the system of particles X_j and derive the equations of motion as the minimization of the action integral subject to fixed initial and final values. This will yield a set of differential equations for the particle trajectories which can then be solved for arbitrary initial conditions.

To derive a formula for the kinetic energy, we need the Shallow Water assumption. The Shallow Water assumption is that the fluid motion is essentially horizontal and that we can therefore ignore the velocity in the vertical direction, i.e., $V^2 \ll U^2$. Thus the kinetic energy of any X_j can be written

$$\tfrac{1}{2} m_j (U_j^2 + V_j^2) \approx \tfrac{1}{2} m_j U_j^2.$$

The kinetic energy of the system is given by

$$KE = \sum_{j=1}^{N} \frac{1}{2} m_j U_j^2 = \frac{1}{2} \sum_{j=1}^{N} m_j \left[\frac{dX_j}{dt} \right]^2, \tag{2.4}$$

where

$$\frac{dX_j}{dt} = U_j. \tag{2.5}$$

We can now derive an expression for the potential energy. We have

$$PE = \int_a^b \int_0^h \rho g y \, dy \, dx = \tfrac{1}{2} \int_a^b g h^2(x) \, dx, \tag{2.6}$$

where g is the gravitation constant and $\rho = 1$. Equation (2.6) can be discretized as

$$PE = \tfrac{1}{2} \sum_{j=1}^{N} g H_j (H_j L_j) = \tfrac{1}{2} \sum_{j=1}^{N} g H_j m_j \qquad \text{using (2.3).}$$

The Lagrangian $L = KE - PE$ is given by

$$L = \frac{1}{2} \sum_{j=1}^{N} \left\{ m_j \left(\frac{dX_j}{dt} \right)^2 - m_j g H_j \right\}. \tag{2.7}$$

Recall that the equations of motion of a mechanical system are derived by minimizing $I = \int_0^T L \, dt$ subject to given initial and final values $X_j(0)$ and $X_j(T)$ [6]. Let

$$I = \int_0^T \frac{1}{2} \sum_{j=1}^{N} m_j \left[\left(\frac{dX_j}{dt} \right)^2 - g H_j \right] dt \tag{2.8}$$

We can now minimize I using the relation $H_j = m_j / L_j$. A necessary condition for a minimum is that

$$\delta I = \delta \left\{ \frac{1}{2} \int_0^T \sum_{j=1}^{N} m_j \left[\left(\frac{dX_j}{dt} \right)^2 - g H_j \right] dt \right\} = 0, \tag{2.9a}$$

where

$$H_j = m_j^0 / L_j. \tag{2.9b}$$

Integrate (2.9a) by parts and use $\delta X_j(0) = \delta X_j(T) = 0$. We have

$$\delta I = \int_0^T \sum_{j=1}^{N} \left[-m_j \frac{d^2 X_j}{dt^2} - \frac{g}{2} \sum_{k=1}^{N} m_k \frac{\partial H_k}{\partial X_j} \right] \delta X_j \, dt = 0. \tag{2.10}$$

Since δX_j is arbitrary, we have, for each j,

$$m_j \frac{d^2 X_j}{dt^2} = -\frac{g}{2} \sum_{k=1}^{N} m_k \frac{\partial H_k}{\partial X_j}. \tag{2.11}$$

We note that $\partial H_k / \partial X_j$ makes sense, since the H_k are functions of $\{X_1, \cdots, X_N\}$ through the relationship $H_k = m_k^0 / L_k$ and $L_k = (X_{k+1} - X_{k-1})/2$.

In fact, we can put Eq. (2.11) into a form that will be more suitable for our numerical method. Using (2.9b) $L_k H_k = m_k^0$, we get

$$\frac{\partial L_k}{\partial X_j} H_k + L_k \frac{\partial H_k}{\partial X_j} = 0.$$

Therefore

$$\frac{\partial H_k}{\partial X_j} = -\frac{H_k}{L_k} \frac{\partial L_k}{\partial X_j}. \tag{2.12}$$

Substituting (2.12) into (2.11) we end up with

$$\begin{aligned} m_j \frac{d^2 X_j}{dt^2} &= \frac{g}{2} \sum_{k=1}^{N} m_k \frac{H_k}{L_k} \frac{\partial L_k}{\partial X_j} \\ &= \frac{g}{2} \sum_{k=1}^{N} (L_k H_k) \frac{H_k}{L_k} \frac{\partial L_k}{\partial X_j} \\ &= \frac{g}{2} \sum_{k=1}^{N} H_k^2 \frac{\partial L_k}{\partial X_j}. \end{aligned} \tag{2.13}$$

In summary, the spatially discrete equations of motion are

$$m_j^0 = L_j H_j \qquad \text{Conservation of Mass,} \tag{2.14a}$$

$$m_j^0 \frac{d^2 X_j}{dt^2} = \frac{g}{2} \sum_{k=1}^{N} H_k^2 \frac{\partial L_k}{\partial X_j} \qquad \text{Conservation of Momentum.} \tag{2.14b}$$

3. Formulas for Derivatives $\partial L_k / \partial X_j$

We now derive a simple formula for the derivatives $\partial L_k / \partial X_j$. If we ignore boundary points, for the moment, we recall the formula for I_k,

$$I_k = \left(\frac{X_{k-1} + X_k}{2}, \frac{X_k + X_{k+1}}{2} \right). \tag{3.1}$$

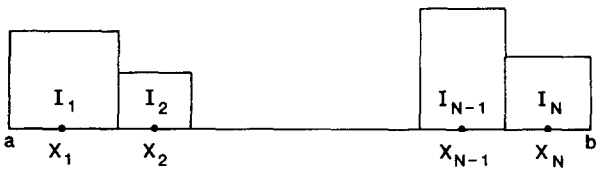

FIG. 3.1. Boundary and neighboring intervals.

Therefore

$$L_k = \frac{X_k + X_{k+1}}{2} - \frac{X_{k-1} + X_k}{2} = \frac{X_{k+1} - X_{k-1}}{2}. \tag{3.2}$$

Thus

$$\begin{aligned} \frac{\partial L_k}{\partial X_j} &= \frac{1}{2}, && j = k+1, \\ &= -\frac{1}{2}, && j = k-1, \\ &= 0 && \text{otherwise.} \end{aligned} \tag{3.3}$$

We can now modify eqs. (3.3) for boundary points. (The boundary points are shown in Fig. 3.1).
The lengths of the boundary intervals are given by

$$L_1 = \frac{X_1 + X_2}{2} - a, \qquad L_N = b - \frac{X_{N-1} + X_N}{2}. \tag{3.4}$$

Equations (3.3) become

$$\begin{aligned} \frac{\partial L_1}{\partial X_j} &= \frac{1}{2}, && j = 1, 2, \\ &= 0 && \text{otherwise,} \\ \frac{\partial L_N}{\partial X_j} &= -\frac{1}{2}, && j = N-1, N, \\ &= 0 && \text{otherwise.} \end{aligned} \tag{3.5}$$

4. Summary of Spatially Discrete Equations of Motion

If we use the formulas (3.3)–(3.5) in Eqs. (2.14a, b) we arrive at the following, spatially discrete, equations of motion:

Conservation of mass.

$$m_1^0 = \left(\frac{X_1 + X_2}{2} - a\right) H_1,$$

$$m_j^0 = \left(\frac{X_{j+1} + X_{j-1}}{2}\right) H_j, \qquad 2 \leqslant j \leqslant N-1,$$

$$m_N^0 = \left(b - \frac{X_{N-1} + X_N}{2}\right) H_N. \tag{4.1}$$

Conservation of momentum.

$$m_1^0 \frac{dU_1}{dt} = \frac{g}{2}\left(\frac{H_1^2 - H_2^2}{2}\right),$$

$$m_j^0 \frac{dU_j}{dt} = \frac{g}{2}\left(\frac{H_{j-1}^2 - H_{j+1}^2}{2}\right), \qquad 2 \leqslant j \leqslant N-1,$$

$$m_N^0 \frac{dU_N}{dt} = \frac{g}{2}\left(\frac{H_{N-1}^2 - H_N^2}{2}\right). \tag{4.2}$$

Move points with local fluid velocity.

$$\frac{dX_j}{dt} = U_j, \qquad 1 \leqslant j \leqslant N. \tag{4.3}$$

5. Relation of Spatially Discrete Equations to Discrete Version of Shallow Water Equations in Lagrangian Form

In this section we show that the spatially discrete equations derived above, Eqs. (4.1)–(4.3), are equivalent to a centered second order accurate finite difference scheme for the shallow water equations in Lagrangian coordinates. We are indebted to Peter Lax for the suggestion that our numerical method should be regarded as a difference scheme in Lagrangian coordinates. This establishes the second order accuracy of the spatial discretization of the polygon method in the continuous (shock-free) regions of the flow.

We remark that this proof does not generalize to higher dimensions, where the order of accuracy is not known [2].

In Eulerian form, the one dimensional shallow water equations are

$$\frac{Dh}{Dt} + h\frac{\partial u}{\partial x} = 0, \tag{5.1a}$$

$$\frac{Du}{Dt} + g\frac{\partial h}{\partial x} = 0, \tag{5.1b}$$

where

$$D = \frac{\partial}{\partial t} + u\frac{\partial}{\partial x},$$

$$h = h(x, t),$$

$$u = u(x, t) \qquad \text{and} \qquad g = \text{constant}.$$

An alternate form of (5.1) is

$$\frac{Dh}{Dt} + h\frac{\partial u}{\partial x} = 0, \tag{5.2a}$$

$$\frac{Du}{Dt} + \frac{g}{2h}\frac{\partial(h^2)}{\partial x} = 0. \tag{5.2b}$$

We now proceed to put (5.2) into Lagrangian form.

In Lagrangian form, our independent variables are **a** and t, where **a** marks a particular fluid element. The flow is described by the family of mappings $X(a, t)$ and by the height $H(a, t)$. Let

$$U(a, t) = \frac{\partial X}{\partial t}(a, t). \tag{5.3}$$

The connection with the Eulerian variables u and h is that

$$\frac{\partial X}{\partial t}(a, t) = u(X(a, t), t), \tag{5.4a}$$

$$H(a, t) = h(X(a, t), t). \tag{5.4b}$$

Note that

$$\begin{aligned}
\frac{\partial}{\partial t}\left(H\frac{\partial X}{\partial a}\right) &= \frac{\partial H}{\partial t}\frac{\partial X}{\partial a} + H\frac{\partial^2 X}{\partial a\,\partial t} \\
&= \frac{\partial H}{\partial t}\frac{\partial X}{\partial a} + H\frac{\partial U}{\partial a} \\
&= \frac{\partial X}{\partial a}\left(\frac{\partial H}{\partial t} + H\frac{\partial U/\partial a}{\partial X/\partial a}\right) \\
&= \frac{\partial X(a, t)}{\partial a}\left(\frac{Dh}{dt} + h\frac{\partial u}{\partial x}\right)\Bigg|_{(X(a,t),t)} \\
&= 0 \qquad \text{by (5.2a).}
\end{aligned}$$

So

$$H\frac{\partial X}{\partial a}=\mu(a) \tag{5.5}$$

independent of t. This is the Lagrangian form of the continuity equation.

We note that $\mu(a)$ is the mass-density with respect to the measure da since $\int_{a_1}^{a_2}\mu(a)\,da=\int_{a_1}^{a_2}H(a,t)\,\partial X(a,t)/\partial a\,da=\int_{X(a_1,t)}^{X(a_2,t)}h(x,t)\,dx=$ mass of the fluid between $X(a_1,t)$ and $X(a_2,t)$. To transform (5.2b) to Lagrangian form, multiply both sides by $\partial X/\partial a$ and use the chain rule to get

$$\frac{\partial X}{\partial a}\frac{\partial^2 X}{\partial t^2}+\frac{g}{2H}\frac{\partial(H^2)}{\partial a}=0. \tag{5.6}$$

Multiply (5.6) by H and use (5.5); we get

$$\mu(a)\frac{\partial^2 X}{\partial t^2}+\frac{g}{2}\frac{\partial(H^2)}{\partial a}=0. \tag{5.7}$$

In summary, the Lagrangian form of the 1-D Shallow Water Equations are

$$H(a,t)=\mu(a)/(\partial X/\partial a) \qquad \text{Conservation of Mass,} \tag{5.8a}$$

$$\mu(a)\frac{\partial U}{\partial t}+\frac{g}{2}\frac{\partial(H^2)}{\partial a}=0 \qquad \text{Conservation of Momentum,} \tag{5.8b}$$

$$\frac{dX}{dt}=U. \tag{5.8c}$$

We now spatially discretize (5.8). Let $a_k=j\Delta a$ and $X_j=X(a_j,t)$, $U_j=U(a_j,t)$ $H_j=H(a_j,t)$. We use a centered, second-order accurate, difference for $\partial/\partial a$

$$\left.\frac{\partial(H^2)}{\partial a}\right|_j=\frac{H_{j+1}^2-H_{j-1}^2}{2\Delta a}. \tag{5.9}$$

Then (5.8) becomes

$$H_j=\mu_j\Big/\left(\frac{X_{j+1}-X_{j-1}}{2\Delta a}\right)=\mu_j\,\Delta a\Big/\left(\frac{X_{j+1}-X_{j-1}}{2}\right), \tag{5.10a}$$

$$\mu_j\frac{dU_j}{dt}+\frac{g}{2}\left(\frac{H_{j+1}^2-H_{j-1}^2}{2\Delta a}\right)=0, \tag{5.10b}$$

$$\frac{dX_j}{dt}=U_j. \tag{5.10c}$$

The Voronoi Polygon Method, away from boundary points, is (4.1)–(4.3)

$$m_j = H_j \frac{(X_{j+1} - X_{j-1})}{2}, \tag{5.11a}$$

$$m_j \frac{dU_j}{dt} + \frac{g}{2}\left[\frac{H_{j+1}^2 - H_{j-1}^2}{2}\right] = 0, \tag{5.11b}$$

$$\frac{dX_j}{dt} = U_j. \tag{5.11c}$$

We recall an earlier remark that μ_j is the mass-density; therefore, the mass of the jth interval is given by

$$m_j = \mu_j \Delta a. \tag{5.12}$$

Thus, using (5.12), the two schemes (5.10) and (5.11) are the same.

6. Shocks

So far what we have described is valid for continuous flows. We can, however, extend this method to treat flows where shocks occur, by the following simple device.

We model a shock as an inelastic collision between two fluid particles. When one particle (say X_2) overtakes another (X_3) and collides with it, we replace them by one averaged particle, X', with velocity and height chosen so that mass and momentum are conserved in the new interval, I', in Fig. 6.1c.

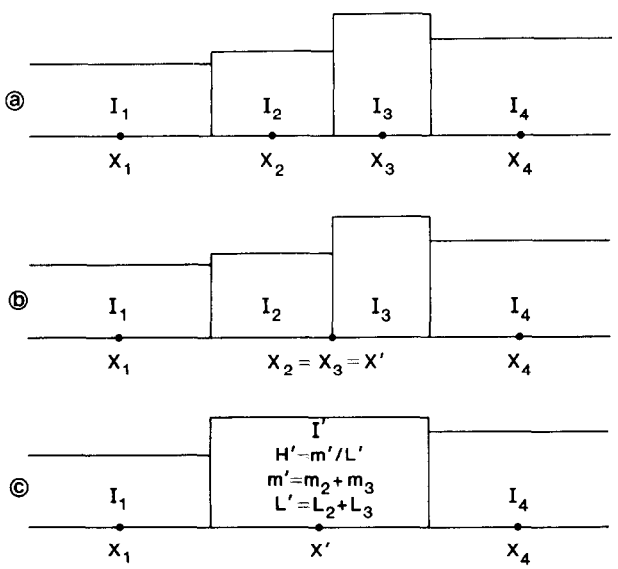

FIGURE 6.1. (a) Points X_2 and X_3 before a continuous-time collision; (b) Points X_2 and X_3 during a continuous-time collision; (c) points X_2 and X_3 after a continuous-time collision.

After a collision has occurred, X_2 and X_3 are replaced by X'. Since the outer boundaries of I_2 and I_3 do not move during a collision there is no transfer of mass or momentum to the noncolliding particles, X_1 and X_4 in Fig. 6.1b, c. This leads to the following equations for conservation of mass and momentum (where primed quantities refer to after collision values),

$$X' = X_2 = X_3, \tag{6.1a}$$

$$L' = L_2 + L_3, \tag{6.1b}$$

$$m' = m_2 + m_3 \qquad \text{Conservation of Mass,} \tag{6.1c}$$

$$m'U' = m_2 U_2 + m_3 U_3 \qquad \text{Conservation of Momentum,} \tag{6.1d}$$

$$H' = m'/L'. \tag{6.1e}$$

We note that when such a collision occurs the total number of fluid markers is decreased by one. This is consistent with the fact that a shock is a dissipative process that results in a loss of information. Thus we require less resolution in those areas where a shock has passed through.

We also remark that one can show (see Appendix) that the total energy decreases after such a collision has occurred. Decreasing energy is the shallow water equivalent of decreasing entropy in gas dynamics.

In actual calculations, and for stability considerations (see Section 7), we cannot allow two particles to actually collide. We therefore consider a collision to take place when two particles (X_2 and X_3 in Fig. 6.2) get closer than some preassigned distance, d. When this happens, we replace X_2 and X_3 by one averaged point X', with velocity and height chosen so that mass and momentum are conserved in the new interval I', and its immediate neighbors X_1 and X_4. A natural choice for the collision distance d will be described in the next section.

We need to determine the position of the new point X' and its velocity U' and mass m'. Since the lengths of I_1 and I_4 (L_1, L_4) are changed by moving X_2 and X_3 to X', we therefore change m_1 and m_4 to m_1' and m_4'. We want the height of H_1 and H_4 to remain the same after the collision, and therefore we adjust m_1', U_1', m_4', U_4', accordingly, to conserve total mass and momentum, as well as the height of noncolliding particles.

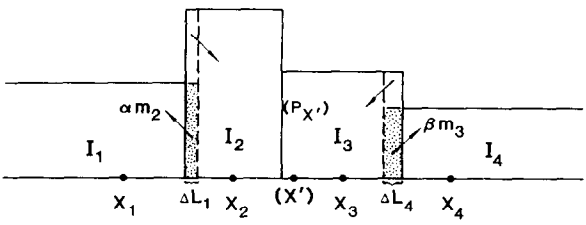

FIG. 6.2. Transfer of fluid mass during a discrete-time collision. Points X_2 and X_3 collide and are merged into X'.

The location of X' is arbitrarily chosen to be a weighted average of X_2 and X_3. Our particular choice, based on numerical experiments, will be described in Section 8.

We arrive at the following system of equations to solve

Conservation of height of non colliding particles

$$H_1' = H_1, \tag{6.2a}$$

$$H_4' = H_4. \tag{6.2b}$$

Conservation of (total) mass

$$m_1' + m' + m_4' = m_1 + m_2 + m_3 + m_4. \tag{6.3}$$

Conservation of (total) momentum

$$m_1'U_1' + m'U' + m_4'U_4' = m_1U_1 + m_2U_2 + m_3U_3 + m_4U_4. \tag{6.4}$$

Create new particle at weighted average of colliding particles

$$X' = \gamma X_2 + (1-\gamma) X_3. \tag{6.5}$$

Mass and Momentum after Collision

The solution of Eqs. (6.2)–(6.5) for the mass and momentum after a collision has occured $(m_1', m', m_4', U_1', U', U_4')$ is not unique. We present a particular, plausible solution constructed according to the following principles.

When X_2 and X_3 are merged into a new point $X_2 \leqslant X' \leqslant X_3$, the boundaries of the intervals I_1' and I_4' are pulled closer to X', thereby increasing the lengths and I_1' and I_4' (L_1', L_4'). We then adjust the masses m_1' and m_4' by adding some of the mass from $I_{X'}$ to I_1' and I_4'. Therefore look for solutions of (6.2)–(6.5) of the form

$$m_1' = m_1 + \alpha m_2, \tag{6.6a}$$

$$m_4' = m_4 + \beta m_3, \tag{6.6b}$$

$$m' = (1-\alpha) m_2 + (1-\beta) m_3. \tag{6.6c}$$

Accordingly, since the new intervals I_1', I_4' represent some of the fluid formerly in I_2 and I_3, which had different velocities, we adjust U_1' and U_4' to account for this.

$$U_1' = \frac{m_1U_1 + \alpha m_2U_2}{m_1 + \alpha m_2}, \tag{6.7a}$$

$$U_4' = \frac{m_4U_4 + \beta m_3U_3}{m_4 + \beta m_3}, \tag{6.7b}$$

$$U' = \frac{(1-\alpha) m_2U_2 + (1-\beta) m_3U_3}{(1-\alpha) m_2 + (1-\beta) m_3}. \tag{6.7c}$$

Conservation of mass and momentum. Before determining α and β, we show that for arbitrary α and β the total mass and momentum are conserved.

Conservation of mass. By Eq. (6.6) we have

$$m_1' + m' + m_4' = (m_1 + \alpha m_2) + [(1-\alpha)\, m_2 + (1-\beta)\, m_3] + (m_4 + \beta m_3)$$
$$= m_1 + m_2 + m_3 + m_4.$$

Conservation of Momentum. By Eq. (6.7) we have

$$m_1' U_1' + m' U' + m_4' U_4' = (m_1 + \alpha m_2) \left(\frac{m_1 U_1 + \alpha m_2 U_2}{m_1 + \alpha m_2} \right)$$
$$+ [(1-\alpha)\, m_2 + (1-\beta)\, m_3)] \left[\frac{(1-\alpha)\, m_2 U_2 + (1-\beta)\, m_3 U_3}{(1-\alpha)\, m_2 + (1-\beta)\, m_3} \right]$$
$$+ (m_4 + \beta m_3) \left[\frac{m_4 U_4 + \beta m_3 U_3}{m_4 + \beta m_3} \right]$$
$$= m_1 U_1 + m_2 U_2 + m_3 U_3 + m_4 U_4$$

Conservation of height of noncolliding particles. We now determine α and β by using Eq. (6.2) (conservation of height of noncolliding particles).

From Fig. 6.2 it can be seen that αm_2 is the portion of m_2 that is transferred from I_2 to I_1, while βm_3 is the portion of m_3 that is transferred from I_3 to I_4 when X_2 and X_3 are merged to X'. We choose α and β so that just enough mass is transferred to I_1' and I_4' to keep the heights H_1' and H_4' unchanged, i.e., $H_1' = H_1$ and $H_4' = H_4$.

$$\alpha m_2 = (\Delta L_1)\, H_1 = \left[\left(\frac{X' + X_1}{2} - \frac{X_2 + X_1}{2} \right) \right] H_1,$$

$$\beta m_3 = (\Delta L_4)\, H_4 = \left[\left(\frac{X_3 + X_4}{2} - \frac{X' + X_4}{2} \right) \right] H_4,$$

so

$$\alpha m_2 = \left(\frac{X' - X_2}{2} \right) H_1, \tag{6.8a}$$

$$\beta m_3 = \left(\frac{X_3 - X'}{2} \right) H_4. \tag{6.8b}$$

Thus the formulas for α and β and hence the other quantities m_1', m', m_4', U_1', U', U_4' are determined once X' is found.

The formula for X' is given by Eq. (6.5) somewhat arbitrarily. Several variants of (6.5) were tried, where we chose X' to satisfy a conservation of center of mass

equation, but that approach led to a quadratic equation for X' which, when tried numerically, did not always have real solutions nor produce better results so we stayed with the simpler formula (6.5). Again, the particular choice of γ in (6.5) will be presented in Section 8.

7. Numerical Method

We now combine the foregoing elements into a numerical method for the 1-D shallow water equations.

The spatially discrete equations in Sections 2 and 3 are

$$m_j = H_j \left(\frac{X_{j+1} - X_{j-1}}{2} \right), \tag{7.1a}$$

$$m_j \frac{dU_j}{dt} = \frac{g}{2} \left(\frac{H_{j-1}^2 - H_{j+1}^2}{2} \right), \tag{7.1b}$$

$$\frac{dX_j}{dt} = U_j, \qquad 2 \leqslant j \leqslant N - 1. \tag{7.1c}$$

We temporally discretize Eq. (7.1) by using a second order Runga-Kutta scheme

$$\tilde{U}_j^{n+1} = U_j^n + (\Delta t) \frac{g}{4m_j} [(H_{j-1}^n)^2 - (H_{j+1}^n)^2], \tag{7.2a}$$

$$\tilde{X}_j^{n+1} = X_j^n + (\Delta t)\, \tilde{U}_j^{n+1}, \tag{7.2b}$$

$$\tilde{H}_j^{n+1} = 2m_j/(\tilde{X}_{j+1}^{n+1} - \tilde{X}_{j-1}^{n+1}). \tag{7.2c}$$

$$U_j^{n+1} = U_j^n + \left(\frac{\Delta t}{2} \right) \left(\frac{g}{4m_j} \right) \{ [(H_{j-1}^n)^2 - (H_{j+1}^n)^2] + [(\tilde{H}_{j-1}^{n+1})^2 - (\tilde{H}_{j+1}^{n+1})^2] \}, \tag{7.3a}$$

$$X_j^{n+1} = X_j^n + \frac{\Delta t}{2} (U_j^n + \tilde{U}_j^{n+1}), \tag{7.3b}$$

$$H_j^{n+1} = 2m_j/(X_{j+1}^{n+1} - X_{j-1}^{n+1}). \tag{7.3c}$$

Note that $\tilde{U}_j^{n+1}$ and U_j^{n+1} are used to update $\tilde{X}_j^{n+1}$, respectively. Nevertheless, the scheme is explicit because $\tilde{U}_j^{n+1}$ and U_j^{n+1} have just been evaluated. Also, U_j^{n+1} can be used in (7.3b) rather than $\tilde{U}_j^{n+1}$ since this quantity is already computed in Eq. (7.3a).

The algorithm is now as follows:

Step 1. Pick N points on the line, with initial velocity U_j and height H_j. This gives the initial mass of each interval I_j,

$$m_j^\circ = L_j^\circ H_j^\circ = (X_{j+1}^\circ - X_{j-1}^\circ)\, H_j^\circ/2.$$

Then store m_j°.

Step 2. Find an intermediate velocity $\tilde{U}_j^{n+1}$ by using (7.2a). Move points with this intermediate velocity to $\tilde{X}_j^{n+1}$, (7.2b), and then calculate intermediate heights $\tilde{H}_j^{n+1}$ by using (7.2c).

Step 3. Calculate new velocity U_j^{n+1} using information from the previous time step and from the computed correction terms (7.2a)–(7.2c).

Step 4. Move points to new locations X_j^{n+1} by (7.3b).

Step 5. Determine new height H_j^{n+1} by using (7.3c).

Step 6. Repeat Steps 2–5 as long as desired.

This algorithm is valid for points not adjacent to the boundary and only for smooth regions of the flow. However, we must modify the algorithm to account for boundary points and shocks. This will be done below.

Before discussing shocks and a boundary treatment, there is another question, that of stability. It is well known, in finite difference calculations for hyperbolic equations, that small perturbations can grow if the Courant–Friedrichs–Lewy (CFL) condition is violated [12], i.e., $\Delta t/\Delta x \leqslant 1/c$, where c is the wave speed appropriate to the problem. For the shallow water equations $c = \sqrt{gH}$. Let $c_{\max} = \max_{1 \leqslant j \leqslant n} \sqrt{gH_j}$ so that, for a fixed Δt, we need

$$\Delta X \geqslant c_{\max}(\Delta t). \tag{7.4}$$

Since our mesh is variable we must examine the CFL condition at each point and therefore we need

$$\min_{1<j<N} (\Delta X)_j^n \geqslant c_{\max}(\Delta t). \tag{7.5}$$

We now have a lower bound on how close two points can get. This forces us to modify the algorithm. After we move the points to their new locations, since they are stored in increasing order ($X_1 < X_2 < X_3 < \cdots$), we sweep through the array containing their locations and see if any two violate the CFL condition (7.5). We must now restore the CFL condition. Since we treat shocks as collisions between particles we cannot, computationally, allow these particles to get closer than the CFL condition allows. If two particles are found to violate the CFL condition, we remove them and replace them by one averaged particle according to the procedure described in the previous section on shocks. We thus reduce the number of computation points by one and move all the stored quantities down one storage location. In this manner we are able to handle shocks while, at the same time, ensure the stability of the computation. We note that this procedure leads to a loss of resolution due to the removal of mesh points. This is in fact what actually happens when a shock passes by. After a shock passes, energy is dissipated and the amount of information required to specify the flow is reduced. This smoothing is manifested by the fact that we now need fewer fluid markers to describe the flow behind a shock. This is consistent with our procedure of treating shocks as collisions between points and merging them into

one averaged point The averaging provides the necessary energy dissipation, and the reduction in the number of fluid markers is consistent with the loss of information.

Boundary treatment—Infinite domain. The method as described above is valid for points interior of the fluid. From a practical point of view, we can only model the region of interest by a finite number of points. Therefore, for an infinite domain, we can only consider a bounded region of fluid. Since the points are indexed in increasing order, the left boundary is the point $a < X_1$ and the right boundary is $b > X_N$. (See Fig. 3.1.) We assume that the region of interest is near $x = 0$ and that **a** and **b** are sufficiently far away from $x = 0$, so that the waves produced at $x = 0$ will not reach the artificial boundaries for a large number of iterations. At that point when the waves produced near $x = 0$ are reflected from the artificial boundaries the computation is no longer valid.

The equations for the points X_1 and X_N are given in Section 4. Since the points X_1 and X_N move, in order to avoid artificial boundary reflections, we need to move the boundaries $X = a$ and $X = b$ at each time step. We present the analysis for the left boundary, but the argument is similar for the right boundary.

Consider the interval I_1. (See Fig. 3.1.) If **a** were fixed and points X_1 and X_2 moved, then the length of I_1 would change. Since the mass of I_1 must be constant, the height H_1 would also change. This would set up artificial waves propagating into the fluid. This can be avoided by keeping the lengths and therefore the height of I_1 constant. We accomplish this by moving **a** with the same velocity as X_1.

$$a^{n+1} = a^n + (\Delta t)\, U_1^{n+1}, \tag{7.6a}$$

$$b^{n+1} = a^n + (\Delta t)\, U_N^{n+1}. \tag{7.6b}$$

This has the effect of computing over a moving region.

Fixed domain. If we are actually interested in a fixed, bounded region of fluid, say $-\infty < a \leqslant x \leqslant b < \infty$, we have to ensure that our fluid markers are confined to the bounded region, i.e., $a < X_i < b$, $i = 1,..., N$. In this case the boundaries are fixed so $a^n = a^0$ and $b^n = b^0$. At each time step we check the points X_1 and X_N to see if they are within CFL of their respective boundaries. If they are, we assume that the particles have had an elastic collision with the wall, and we reverse their velocities. If a particle passes out of the region during a time step, we reflect it back in and reverse its velocity.

8. Results

In this section we present some numerical results for the problem of the breaking of a dam. The initial conditions are illustrated in Fig. 8.1.

At time $t = 0$ the dam is suddenly destroyed and the problem is to determine the subsequent motion of the water for x and t.

Note that this problem is analogous to the Riemann problem of one-dimensional

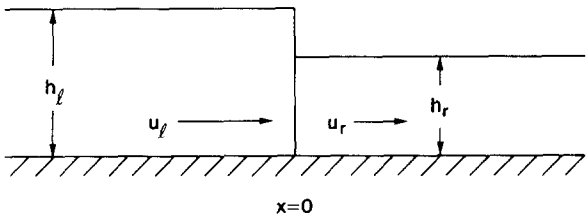

FIG. 8.1. Initial conditions for Dam-Breaking problem.

gas dynamics (see Courant and Friedrichs [3]). The initial conditions we have used are those for which the exact solution is provided in Stoker [14],

$$\begin{aligned} u(x,0) &= 0.2667 \text{ m/sec}, && x < 0, \\ &= 1.6\ m/\text{sec}, && x > 0. \end{aligned} \tag{8.1a}$$

$$\begin{aligned} h(x,0) &= 10.8 \text{ m}, && x < 0, \\ &= 1.8 \text{ m}, && x > 0. \end{aligned} \tag{8.1b}$$

The exact solution consists of four regions (see Fig. 8.2). A shock wave (or bore) propagates into the constant state (region IV) with velocity 10.7 m/sec. Behind the shock (region III) is a simple wave where the height is constant. Region II is a rarefaction wave which connects the constant height state (region III) with the undisturbed fluid in region I.

At any time the height of the fluid is

$$\begin{aligned} h(x,t) &= 10.8 \text{ m}, && x > 10.7t, \\ &= 4.716 \text{ m}, && 0.45t \leqslant x \leqslant 10.7t, \\ &= \frac{1}{88.2}\left(20.8401 - \frac{x}{t}\right)^2 \text{m}, && -10.02t \leqslant x \leqslant 0.45t, \\ &= 10.8 \text{ m}, && x \leqslant -10.02t. \end{aligned}$$

In Figs. 8.3 we present the results of our calculations for the following parameters: $\Delta t = 0.2$, $\Delta X = 5$ meters (initially), and the merging parameter $d = 2$ meters. We

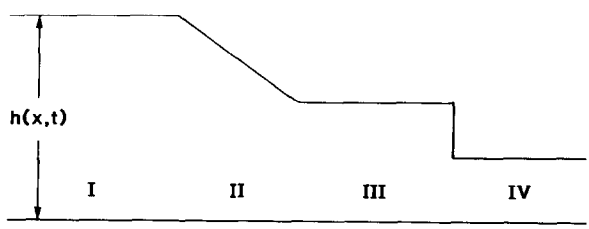

FIG. 8.2. Exact solution of Dam-Breaking problem.

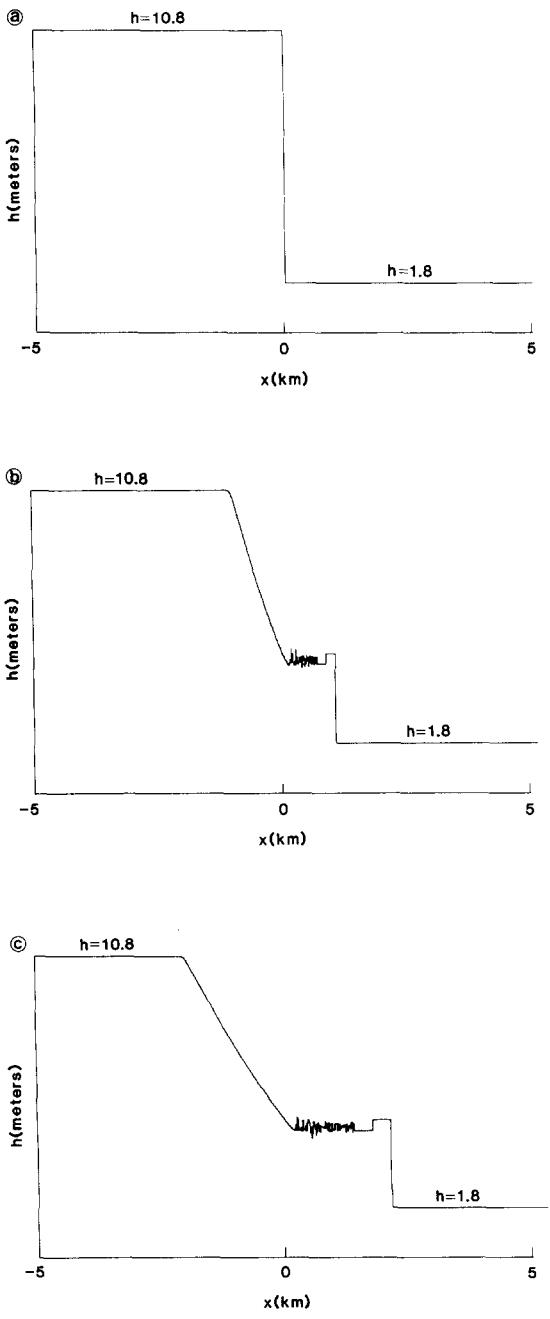

FIG. 8.3. Computed solutions for Dam-Breaking problem for (a) $t = 0$ sec, (b) $t = 100$ sec, (c) $t = 200$ sec, (d) $t = 300$ sec, (e) $t = 400$ sec, (f) $t = 450$ sec. Exact solution (in dark lines) superimposed on computed solution at each fluid marker.

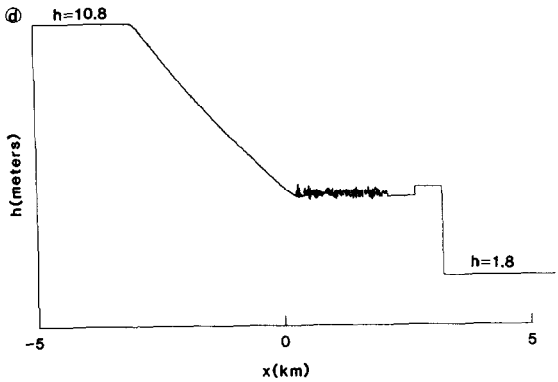

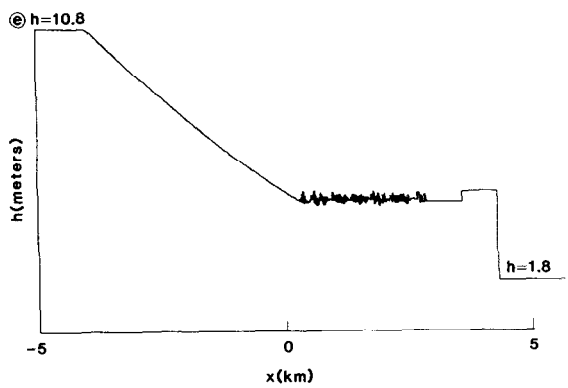

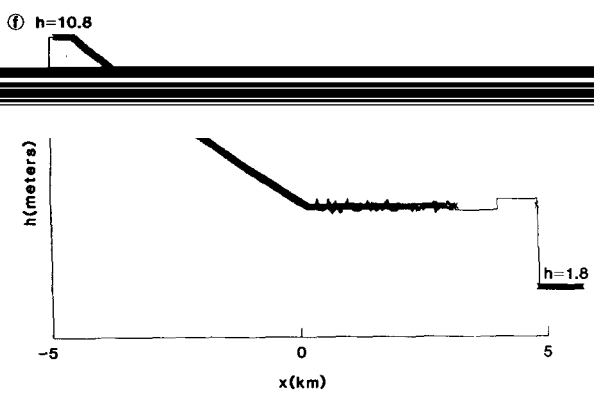

FIG. 8.3—*Continued.*

follow the shock for 5 km and plot every 100 sec (i.e., 500 iterations). In the last plot we superimpose the exact solution (dark X's) on top of the computed solution.

One feature of our solution is that the shock and rarefaction waves are sharp and in the right place. As shown in Figs. 8.3, the method gives particularly sharp fronts and very exact shock speeds. There is a slight overshoot in the height immediately behind the shock and there are small oscillations in the constant state (region III) near the rarefaction wave. These oscillations are small, however, and remain small throughout the calculation.

An interesting observation is that there is a region behind the shock in which there are no fluid markers. In this region the flow is constant. It is observed from numerical experiment that the distribution of points in the constant state (region III) and the presence of large oscillations immediately behind the shock is sensitive to the merging procedure. Since we do not use an artificial viscosity term of the von Neuman–Richtmyer type [12] the only dissipation we have, is introduced by the merging procedure (see Appendix). It is important that we pick the new point X' so that enough dissipation is introduced to smooth out the oscillations behind the shock. In the author's previous work [1] this was not done entirely satisfactorily and there were oscillations behind the shock. In that work we used a first order Euler difference and X' was placed at the center of mass of the two colliding points, i.e.,

$$X' = \frac{m_k X_k + m_{k+1} X_{k+1}}{m_k + m_{k+1}}.$$

In the present work we have switched to a second order Runge-Kutta type scheme and have changed the location of X'. We now place X' upstream of the shock, i.e.,

$$X' = \gamma X_k + (1 - \gamma) X_{k+1},$$

where $\gamma = 0$ for a right propagating shock and $\gamma = 1$ for a left propagating shock. This combination of using a second order method plus the new merging procedure seems to introduce the right amount of dissipation to get rid of the oscillations immediately behind the shock. The way it does this is by bunching more points into the back part of the constant state while leaving very few points in the front part, immediately behind the shock. The result is, that this region is represented by very few points, and is thus constant. Again, this is consistent with the notion of a shock as a smoothing process. Therefore, once a shock passes, you need less points to represent the flow. The reason that this particular choice of X' in combination with a second order method is needed to achieve these results is still unclear.

We note that the same problem has been solved by Marshall and Mendez [10] using the Glimm–Chorin Random Choice method. In their solution the shock wave and depression (rarefraction) wave are computed with almost infinite resolution. The location of the shock and depression wave, however, is not exact. The constant state in [10] appears, exact, while the depression wave is very close to the exact solution.

In our solution, the location of the shock and depression wave appears to agree

with the theoretical solution very closely. The depression wave is also very close. The constant state is not constant, but (in a region not adjacent to the shock) oscillates about the correct height with small oscillations that remain small in time. It should be pointed out that the random choice method uses the exact solution to the Riemann problem in its numerical construction of an approximate solution. Thus it makes use of the exact solution of the Riemann problem to solve the Riemann problem as a test case. This criticism does not apply to the present method.

9. Conclusion

We have presented a Lagrangian method for the numerical solution of the shallow water equations in one space dimension based on a Voronoi mesh. Initial results for the Dam-Breaking problem, show the method to be promising. By introducing a conservative merging procedure for colliding particles we are able to handle the weak shocks that occur in shallow water type problems.

This method, however, was originally developed by the author to handle problems dealing with flows on a rotating sphere that arise in atmospheric modelling. The details of the 2-D spherical method will be presented in a subsequent paper [2]. We briefly mention some of the features of the 1-D method that have to be modified in a 2-D treatment.

In 2-D it is possible that points can be brought close enough to collide and trigger the merging algorithm, without shocks being present, i.e., in strong shearing flows. Therefore, we will introduce a simple test so that points are only merged when the collisions are compressive and not when they are caused by shearing.

Also, in 2-D the Voronoi cell boundaries are not strictly Lagrangian, even though the fluid markers are, and this introduces a flux across the cell boundaries that does not occur in 1-D.

Finally, the grid construction and its associated data structure are considerably more complicated in 2-D, than they are in the trivial 1-D case. An efficient construction of the Voronoi mesh on a sphere along with its associated data structure, will also be given.

Appendix

Energy Relations. In this section we discuss the energy relations for the scheme. Specifically, we show that the method conserves energy in the absence of shocks, and that energy decreases in the presence of shocks. This analysis will be limited to the discrete-space continuous-time version of the method, however.

Following the notation of Section 5, the discrete equations can be written in the form

$$\mu(a_k)\frac{\partial^2 X_k}{\partial t^2}+\frac{1}{2}\rho g\left[\frac{H_{k+1}^2-H_{k-1}^2}{2\Delta a}\right]=0, \tag{A.1}$$

$$\rho H_k\frac{(X_{k+1}-X_{k-1})}{2\Delta a}=\mu(a_k), \tag{A.2}$$

where $a_k=k\Delta a$, $\mu(a)$ is the mass-density function and $\rho=$ fluid density.

Conservation of Energy. Let

$$U_k=\frac{\partial X_k}{\partial t}. \tag{A.3}$$

Then (A.2) implies

$$\rho\frac{\partial H_k}{\partial t}\frac{X_{k+1}-X_{k-1}}{2\Delta a}+\rho H_k\frac{U_{k+1}-U_{k-1}}{2\Delta a}=0. \tag{A.4}$$

Multiply (A.4) by H_k and use (A.2) again

$$\mu(a_k)\frac{\partial H_k}{\partial t}+\rho H_k^2\frac{U_{k+1}-U_{k-1}}{2\Delta a}=0. \tag{A.5}$$

Now multiply (A.1) by $U_k\Delta a$ and sum over k,

$$\frac{d}{dt}\left(\frac{1}{2}\sum_k\mu(a_k)\Delta a U_k^2\right)+\frac{1}{2}\rho g\sum_k\Delta a U_k\left[\frac{H_{k+1}^2-H_{k-1}^2}{2\Delta a}\right]=0, \tag{A.6}$$

$$\frac{d}{dt}\left(\frac{1}{2}\sum_k\mu(a_k)\Delta a U_k^2\right)-\frac{1}{2}\rho g\sum_k\Delta a\left[\frac{U_{k+1}-U_{k-1}}{2a}\right]H_k^2=0. \tag{A.7}$$

Using (A.5) and (A.7) we get

$$\frac{d}{dt}\sum_k\left[\frac{1}{2}\mu(a_k)U_k^2+\frac{g}{2}\mu(a_k)H_k\right]\Delta a=0. \tag{A.8}$$

Therefore

$$\begin{aligned}E&=\sum_k\Delta a\left[\frac{1}{2}\mu(a_k)U_k^2+\frac{g}{2}\mu(a_k)H_k\right]\\&=\sum_k\left[\frac{1}{2}m_kU_k^2+\frac{g}{2}m_kH_k\right].\end{aligned} \tag{A.9}$$

is conserved.

Shocks. We assume that particles X_K and X_{K+1} actually collide at time $t = T$, therefore $X_K = X_{K+1}$. We then delete the point $K+1$ and lower all subsequent indices by 1. Specifically, let

$$\begin{aligned} X'_k &= X_k, && k \leqslant K, \\ &= X_{k+1}, && k > K, \end{aligned} \tag{A.10}$$

$$\begin{aligned} \mu'(a_k) &= \mu(a_k), && k < K, \\ &= \mu(a_k) + \mu(a_{k+1}), && k = K, \\ &= \mu(a_{k+1}), && k > K, \end{aligned} \tag{A.11}$$

$$\begin{aligned} U'_k &= U_k, && k < K, \\ &= [\mu_k U_k + \mu_{k+1} U_{k+1}]/\mu'(a_k), && k = K, \\ &= U_{k+1}, && k > K. \end{aligned} \tag{A.12}$$

The formula for H' can be derived from (A.2). The result is

$$\begin{aligned} H'_k &= H_k, && k < K, \\ &= \frac{H_k(X_k - X_{k-1}) + H_{k+1}(X_{k+2} - X_k)}{(X_k - X_{k-1}) + (X_{k+2} - X_k)}, && k = K, \\ &= H_{k+1}, && k > K. \end{aligned} \tag{A.13}$$

Note that

$$X_k = X_{k+1}.$$

We want to show that the energy is decreased by this procedure. First consider the kinetic energy

$$\begin{aligned} E'_{\text{Kin}} - E_{\text{Kin}} &= \frac{\Delta a}{2}\left[\mu_K (U'_K)^2 - \mu_K U_K^2 - \mu_{K+1} U_{K+1}^2\right], \\ &= \frac{\Delta a}{2}\left[\frac{(\mu_K U_K + \mu_{K+1} U_{K+1})^2}{\mu_K + \mu_{K+1}} - \mu_K U_K^2 - \mu_{K+1} U_{K+1}^2\right], \\ &= \frac{-\Delta a}{2(\mu_K + \mu_{K+1})} \mu_K \mu_{K+1} (U_K - U_{K+1})^2 < 0. \end{aligned} \tag{A.14}$$

Next, consider the potential energy

$$E'_{\text{Pot}} - E_{\text{Pot}} = \frac{g\Delta a}{2}(\mu'_K H'_K - \mu_K H_K - \mu_{K+1} H_{K+1}). \tag{A.15}$$

Recall (Section 5) that $\mu_k \Delta a = \rho H_k L_k$, where

$$L_k = \frac{X_{k+1} - X_{k-1}}{2},$$

and also that

$$H'_K L'_K = H_K L_K + H_{K+1} L_{K+1},$$
$$L'_K = L_K + L_{K+1}.$$

Therefore

$$E'_{\text{Pot}} - E_{\text{Pot}} = \frac{\rho g}{2} (L'_K H'^2_K - L_K H_K^2 - L_{K+1} H_{K+1}^2). \tag{A.16}$$

The same manipulations as in the kinetic energy case show that

$$E'_{\text{Pot}} - E_{\text{Pot}} = \frac{-\rho g}{2} \frac{L_K L_{K+1}}{L_K + L_{K+1}} (H_k - H_{K+1})^2 < 0. \tag{A.17}$$

We remark that it has been verified numerically that similar results hold for the discrete-time discrete-space case, i.e., energy decreases when we merge points according to the procedure described in Section 6.

ACKNOWLEDGMENTS

This research was initiated and carried out under the direction of Charles Peskin as part of the author's Ph.D. thesis. It is a pleasure to acknowledge the discussions and comments of S. Childress, M. Ghil, E. Isaacson, and P. Lax. The computations were supported by the U.S. Department of Energy under contract DE-AC02-76ER03077 at the Courant Mathematics and Computing Laboratory of New York University.

REFERENCES

1. J. AUGENBAUM, "A New Lagrangian Method for the Shallow Water Equations," Ph.D. thesis, New York University, 1982.
2. J. AUGENBAUM, "A New Lagrangian Method for the Shallow Water Equations—Flows on a Rotating Sphere," submitted.
3. R. COURANT AND R. FRIEDRICHS, "Supersonic Flow and Shock Waves," Interscience, New York, 1948.
4. J. DUKOWICZ, *in* "Numerical Methods for Coupled Problems," Pineridge Press, Swansea, England, 1981.
5. M. S. FRITTS AND J. P. BORIS, *J. Comput. Phys.* **31** (1979), 173.
6. H. GOLDSTEIN, "Classical Mechanics," Addison–Wesley, Reading, Mass., 1950.
7. F. H. HARLOW, *Proc. Symp. Appl. Math.* **15** (1963), 269.
8. C. W. HIRT, A. A. AMSDEN, AND J. L. COOK, *J. Comput. Phys.* **14** (1974), 227.

9. P. D. LAX, "Hyperbolic Systems of Conservation Laws and the Mathematical Theory of Shocks Waves," SIAM, Philadelphia, 1973.
10. G. MARSHALL AND R. MENDEZ, *J. Comput. Phys.* **39** (1981), 1.
11. C. S. PESKIN, A Lagrangian method for the Navier–Stokes equations with large deformations, preprint.
12. R. O. RICHTMYER AND K. W. MORTON, "Finite Difference Method for Initial Value Problems," Interscience, New York, 1967.
13. G. SOD, *J. Comput. Phys.* **27** (1978), 1.
14. J. J. STOKER, *Commun. Pure Appl. Math.* **1** (1948), 1.
15. J. J. STOKER, "Water Waves," Interscience, New York, 1957.
16. H. E. TREASE, "A Two Dimensional Free Lagrangian Hydrodynamics Model", Ph.D. thesis, University of Illinois at Urbana–Champaign, 1981.
17. G. VORONOI, *J. Reine Angew. Math.* **134** (1908), 198.